

Searches for Higgs and BSM at the Tevatron

Arnaud Duperrin ^a

CPPM, IN2P3-CNRS, Université de la Méditerranée, F-13288 Marseille, France
e-mail: duperrin@cppm.in2p3.fr

October 23, 2007

Abstract. This paper presents an overview of recent experimental direct searches for Higgs-boson and beyond-the-standard-model (BSM) physics shown in the plenary session at the SUSY07 conference. The results reported correspond to an integrated luminosity of up to 2 fb^{-1} of Run II data from $p\bar{p}$ collisions collected by the CDF and DØ experiments at the Fermilab Tevatron Collider. Searches covered include: the standard model (SM) Higgs boson (including sensitivity projections), the minimal supersymmetric extension of the standard model (MSSM), charged Higgs bosons and extended Higgs models, supersymmetric decays that conserve R -parity, gauge-mediated supersymmetric breaking models, long-lived particles, leptoquarks, extra gauge bosons, extra dimensions, and finally signature-based searches. Given the excellent performance of the collider and the continued productivity of the experiments, the Tevatron physics potential looks very promising for discovery in the coming larger data sets. In particular, the Higgs boson could be observed if its mass is light or near 160 GeV.

PACS. 1 4.80.Bn, 14.80.Cp, 14.80.Ly, 12.60.Jv, 12.60.Cn, 12.60.Fr, 13.85.Rm

1 Introduction

The standard model is a successful model which predicts experimental observables at the weak scale with high precision. However, the electroweak symmetry breaking mechanism by which weak vector bosons acquire non-zero masses remains an outstanding issue of elementary particle physics. The simplest mechanism involves the introduction of a complex doublet of scalar fields that generate particle masses via their mutual interactions, leading to the so-called SM Higgs boson with an unpredicted mass [1]. Furthermore, the SM fails to explain, for instance, cosmological phenomena like the nature of dark matter in the universe. These outstanding issues are strong evidence for the presence of new physics beyond the standard model. Among the possible extensions of the standard model, supersymmetric (SUSY) models [2] provide mechanisms allowing for the unification of interactions and a solution to the hierarchy problem. Particularly attractive are models that conserve R -parity, in which SUSY particles are produced in pairs and the lightest supersymmetric particle (LSP) is stable. In supergravity-inspired models (SUGRA) [3], the lightest neutralino $\tilde{\chi}_1^0$ arises as the natural LSP, and, being neutral and weakly interacting, could be responsible for the dark matter in the universe.

This paper reports recent experimental results of direct searches for the Higgs boson and BSM physics based on data collected by the CDF and DØ collabora-

tions at the Fermilab Tevatron collider [4]. The dataset analyzed corresponds to an integrated luminosity of up to 2 fb^{-1} . More details on the analyses can be found in Ref. [5,6] and in the proceedings corresponding to the parallel-session presentations.

Table 1. Run II luminosity delivered by the Tevatron accelerator, and luminosity recorded by the DØ experiment in summer 2007.

	Delivered	Recorded
Run IIa	1.6 fb^{-1}	1.3 fb^{-1}
Run IIb	1.7 fb^{-1}	1.5 fb^{-1}
Total	3.3 fb^{-1}	2.8 fb^{-1}

2 The Tevatron Accelerator

The Tevatron is performing extremely well. For Run II, which started in March 2001, a series of improvements were made to the accelerator to operate at a center-of-mass energy of 1.96 TeV with a bunch spacing of 396 ns. Before the 2007 shutdown, monthly integrated and peak luminosities of up to 167 pb^{-1} and $2.86 \times 10^{32} \text{ cm}^{-2} \text{ s}^{-1}$ respectively have been achieved. The consequence, in terms of numbers of interactions per crossing is that the Tevatron is already running in a mode similar that expected at the Large Hadron

^a for the CDF and DØ collaborations

Collider (LHC). The $D\bar{O}$ integrated luminosity delivered and recorded, since the beginning of Run II, is given in Table 1, with similar values for CDF.

3 The CDF and $D\bar{O}$ Experiments

A full description of the CDF and $D\bar{O}$ detectors is available in Ref. [7, 8]. Both experiments are in a steady state of running and take data with an average efficiency of 85%. An upgrade of the detectors to improve the detector capabilities for the Run IIb of the Tevatron was successfully concluded in 2006. The $D\bar{O}$ upgrade included the challenging insertion of an additional layer of radiation-hard silicon detector (L0) to improve the tracking performance. CDF and $D\bar{O}$ completed calorimeter and tracker trigger upgrades to significantly reduce the jet, missing energy, and di-electron trigger rates at high luminosity, while maintaining good efficiency for physics.

4 Standard Model Higgs Boson

Of particular interest is the search for the standard model Higgs boson because this fundamental ingredient of the theory has not been observed and could be reachable at the Tevatron if its mass is light or near 160 GeV. Furthermore, exploiting the theory relationships and the precision electroweak measurements allows to constraint the mass m_H of the Higgs boson. Taking both the experimental and the theoretical uncertainties into account, the indirect upper limit is set at $m_H < 182$ GeV [9] when including the lower limits $m_H > 114.4$ GeV [10] from direct $e^+e^- \rightarrow Z^* \rightarrow ZH$, with both limits set at 95% confidence level (C.L).

Due to the large branching fraction of the Higgs boson into $b\bar{b}$ at low masses ($m_H < 135$ GeV), only the associated Higgs production channels can be disentangled from the multijet $b\bar{b}$ background by exploiting the leptons and the missing transverse energy in the final state. At high mass ($m_H \sim 160$ GeV), the branching fraction is mainly into WW boson pairs, leading to a favorable environment for the analysis with a final state with two leptons and two neutrinos.

Given the low signal production cross section for a SM Higgs boson, CDF and $D\bar{O}$ maximize their global sensitivity by taking advantage of more than 10 different final states, including hadronic taus in W decay, before combining their results.

Both CDF and $D\bar{O}$ use similar search strategies based on a neural network discriminant or likelihoods ratio constructed from matrix-element probabilities. As an illustration for these searches, Fig. 1 shows the distributions of the final variables used by the $D\bar{O}$ experiment for the combination between the different channels corresponding to associated production ($WH \rightarrow \ell\nu b\bar{b}$, $ZH \rightarrow \ell\ell/\nu\nu b\bar{b}$). The distribution of the likelihood ratio discriminator is represented in Fig. 2 and the numbers of expected and observed events are

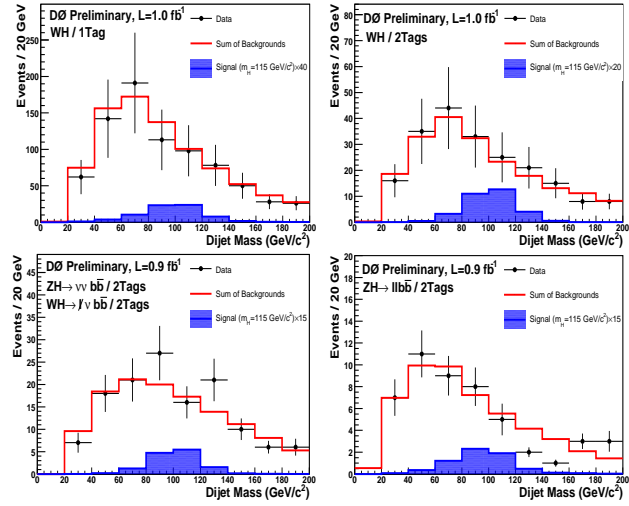


Fig. 1. The final analysis variable distributions for associated Higgs boson production searches by the $D\bar{O}$ experiment. The figure contains the dijet invariant mass distributions for: the $WH \rightarrow \ell\nu b\bar{b}$ analysis after requiring one (a) or two (b) b -tagged jets, the dijet invariant mass for the $ZH \rightarrow \nu\bar{\nu} b\bar{b}$ analysis (c), and for the $ZH \rightarrow \ell\ell b\bar{b}$ analysis (d). The ZH analyses require two b -tagged jets. For each figure, the total background expectations and the observed data are shown. The expected Higgs signals at $m_H = 115$ GeV are scaled as indicated.

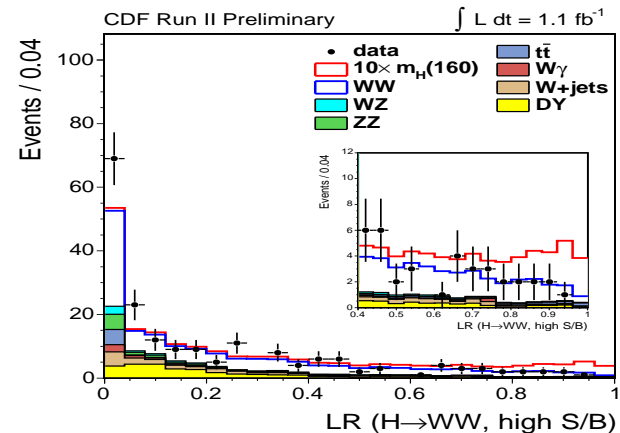


Fig. 2. The distribution of the likelihood ratio (LR) discriminator in a high signal (S) over background (B) region for the Higgs boson in the $H \rightarrow W^+W^-$ decay channel. The expected SM backgrounds and observed data are shown. The expected Higgs signal at $m_H = 160$ GeV is scaled as indicated.

shown in Table 2 for the gluon fusion ($H \rightarrow W^+W^-$) analyses performed by the CDF experiment.

The cross section limits on SM Higgs boson production $\sigma \times BR(H \rightarrow X)$ obtained by combining CDF and $D\bar{O}$ results are displayed in Fig. 3 (left). The result is normalized to the SM cross section: a value of 1 would indicate a Higgs mass excluded at 95% C.L. The observed upper limits are a factor of 10.4 (3.8) higher than the expected cross section for $m_H = 115$ (160) GeV

Table 2. The numbers of signal events expected for a Higgs boson mass $m_H = 160$ GeV, events expected from SM backgrounds, and data events observed, for the CDF experiment. The SM Higgs boson production and decay are assumed to be $gg \rightarrow H \rightarrow WW^* \rightarrow l^+l^- \nu\nu$, where $l^\pm = e, \mu$, or τ . The final state $e trk$ (μtrk) require an electron (a muon) and an additional track.

Category	Higgs ($m_H = 160$ GeV)	WW	WZ	ZZ	$t\bar{t}$	DY	$W\gamma$	W+jets	Total	Data
$e e$	0.7	24.4	3.0	4.6	1.6	13.0	11.6	13.8	72.2 ± 6.1	75
$e \mu$	1.6	58.6	1.7	0.3	4.1	13.1	10.1	16.4	104.3 ± 9.3	113
$\mu \mu$	0.6	19.0	2.3	3.7	1.6	21.0	0.0	3.1	50.6 ± 5.2	56
$e trk$	0.6	20.1	1.5	1.9	1.5	5.3	2.7	5.6	38.6 ± 2.8	47
μtrk	0.4	10.8	0.9	1.3	0.8	2.8	0.3	3.5	20.4 ± 1.5	32
Total	3.9	132.9	9.5	11.7	9.6	55.4	24.7	42.4	286.1 ± 23.3	323

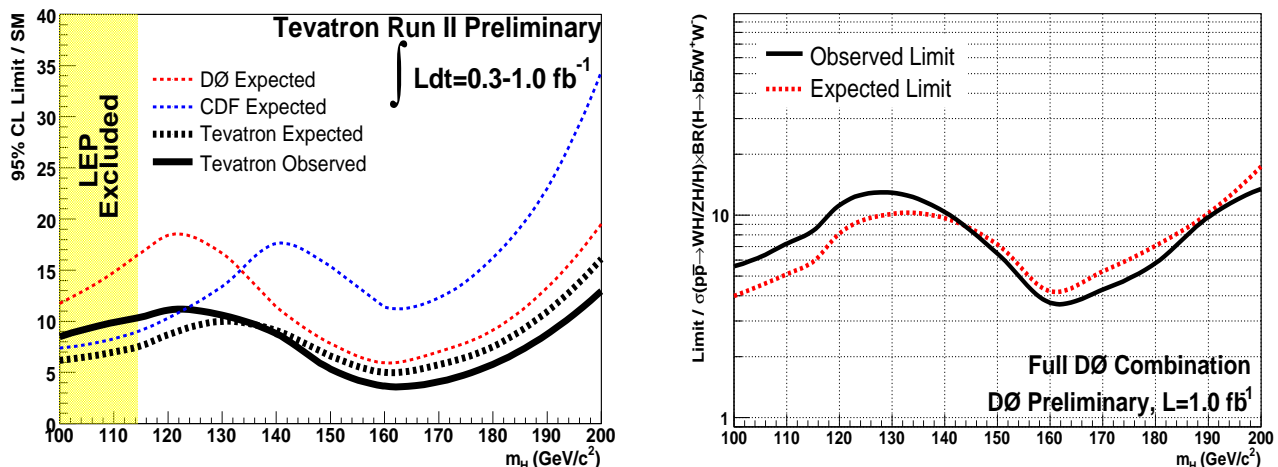


Fig. 3. Left plot (July 2006): upper bound on the SM Higgs boson cross section obtained by combining CDF and DØ results as a function of the Higgs boson mass. The contributing production processes include associated production ($WH \rightarrow \ell\nu b\bar{b}$, $ZH \rightarrow \ell\ell/\nu\nu b\bar{b}$, $WH \rightarrow WW^+W^-$) and gluon fusion ($H \rightarrow W^+W^-$). The limits at 95% confidence level (C.L) are shown as a multiple of the SM cross section. The solid curve shows the observed upper bound, while the dashed curves show the expected upper bounds assuming no signal is present. Analyses are conducted with integrated luminosities ranging from 0.3 fb^{-1} to 1.0 fb^{-1} recorded by each experiment. The region excluded by the LEP experiments is also displayed in the figure [10]. Right plot (March 2007): expected and observed 95% C.L cross section ratios for the combined $WH/ZH/H, H \rightarrow b\bar{b}/W^+W^-$ analyses in the $m_H = 100 - 200$ GeV mass range for DØ alone.

with $0.3\text{-}1.0 \text{ fb}^{-1}$ collected at CDF and DØ. The corresponding expected upper limits are 7.6 (5.0).

Since the first CDF and DØ combination in 2006, a lot of progress has been made resulting in better sensitivity in all channels: neural-net b -tagger, improved selection, matrix-element techniques, etc. Many of these improvements lead to an equivalent gain of more than twice the luminosity, which means that the sensitivity has progressed faster than one would expect from the square root of the luminosity gained. The improved sensitivity from DØ alone is given in Fig. 3 (right).

5 SM Higgs Boson Prospects

Recent projections in sensitivity have been made based on achievable improvements of the current analyses. These include progress on the usage of the existing taggers and of upgraded triggers acceptance, increased

usage of advanced analysis techniques, jet resolution optimization, inclusion of additional channels in the combination, or b -tagging enhancement from the DØ Layer 0.

With the Tevatron running well, up to ~ 6 SM Higgs events/day are produced per experiment and the CDF and DØ collaborations constantly improve their ability to find them. Combining CDF and DØ, about $3\text{-}4 \text{ fb}^{-1}$ could be sufficient to exclude at 95% C.L the SM Higgs boson for $m_H = 115$ GeV and $m_H = 160$ GeV. Assuming 7 fb^{-1} of data analyzed by the end of the Tevatron running, all SM Higgs boson masses except for the real mass value could be excluded at 95% C.L up to 180 GeV.

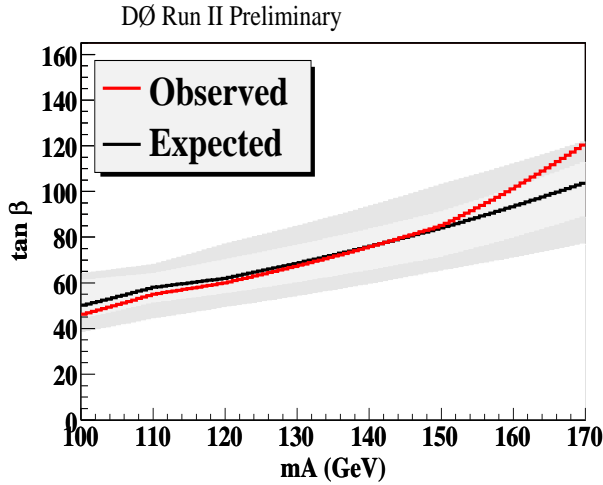


Fig. 4. The MSSM exclusion limit at 95% C.L. obtained by the D0 experiment on searches for neutral Higgs bosons produced in association with bottom quarks and decaying into $b\bar{b}$, projected onto the $(\tan\beta, m_A)$ plane of the parameter space, assuming $\tan^2\beta$ cross section enhancement. The error bands indicate the $\pm 1\sigma$ and $\pm 2\sigma$ range of the expected limit.

6 Higgs Bosons in the MSSM

In the minimal supersymmetric extension of the standard model, two Higgs doublets are necessary to cancel triangular anomalies and to provide masses to all particles. After electroweak symmetry breaking, the MSSM predicts 5 Higgs bosons. Three are neutral bosons: h , H (scalar) and A (pseudo-scalar), and two are charged bosons: H^+ and H^- . An important prediction of the MSSM is the theoretical upper limit $m_h < 135$ GeV on the mass of the lightest Higgs boson. The main difference between the MSSM Higgs bosons and the SM Higgs boson is the enhancement of the cross section production by a factor proportional to $\tan^2\beta$, where $\tan\beta = v_2/v_1$ is the ratio of the vacuum expectation values associated with the neutral components of the two Higgs fields. At tree level, only the mass m_A and $\tan\beta$ are necessary to parameterize the Higgs sector in the MSSM. For $\tan\beta > 1$, decays of h and A to $b\bar{b}$ and $\tau^+\tau^-$ pairs are dominant with branching fraction of about 90% and 8%, respectively. Although most of the experimental searches at Tevatron assume CP conservation (CPC) in the MSSM sector, CP -violating effects can lead to sizable differences for the production and decay properties of the Higgs bosons compared to the CPC scenario.

At the Tevatron, CP invariance is assumed for the searches. The D0 experiment has presented results with 1 fb^{-1} on searches for neutral Higgs bosons produced in association with bottom quarks and decaying into $b\bar{b}$. The currently excluded domain is shown in Fig. 4. For the gluon fusion process $gg \rightarrow h, H, A$, only the $\tau^+\tau^-$ mode is promising due to the overwhelming $b\bar{b}$ background. The preliminary limits from CDF and D0 are available in the $(\tan\beta, m_A)$ plane and are usually summarized for two SUSY scenarios [11]. The

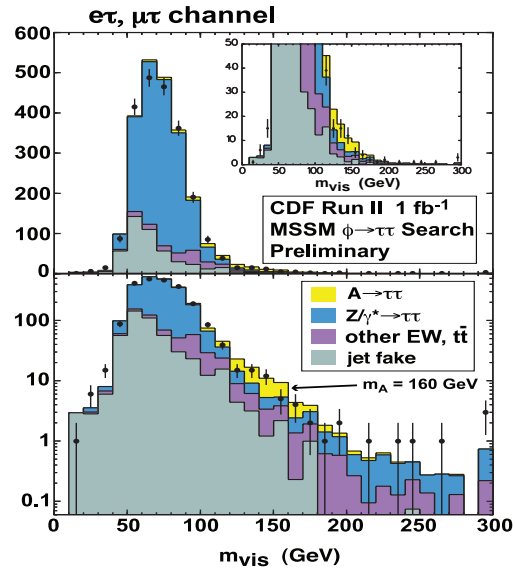


Fig. 5. Partially reconstructed di-tau mass ($M_{vis} = \sqrt{p_{T\mu} + p_{T\tau} + \cancel{E}_T}$) of the CDF search for neutral MSSM Higgs boson production in the $\tau^+\tau^-$ final state. Data (points with error bars) and expected backgrounds (filled histogram) are compared. The expected contribution from a signal at $m_A = 160$ GeV is shown.

m_h^{max} scenario is designed to maximize the allowed values of m_h and therefore yields conservative exclusion limits. The no-mixing scenario differs by the value (set to zero) of the parameter which controls the mixing in the stop sector, and hence leads to better limits. Figure 5 shows the CDF search in the $\tau^+\tau^-$ final state based on 1 fb^{-1} .

7 Charged Higgs Bosons

Charged Higgs bosons are predicted in the MSSM and could be produced in the decay of the top quark $t \rightarrow bH^+$, which would compete with the SM process $t \rightarrow bW^+$.

Doubly-charged Higgs bosons are predicted in many scenarios, such as left-right symmetric models, Higgs triplet models and little Higgs models [12, 13]. The recent D0 search for $H^{\pm\pm}$ in the $\mu^+\mu^+\mu^-\mu^-$ final state using 1 fb^{-1} set preliminary lower bounds limits for right- and left-handed $H^{\pm\pm}$ bosons at 126 GeV and 150 GeV respectively at 95% C.L.

8 Extended Higgs Models

In a more general framework, one may expect deviations from the SM predictions to result in significant changes in the Higgs boson discovery signatures. One such example is the so-called ‘fermiophobic’ Higgs boson, which has suppressed couplings to all fermions. Experimental searches for fermiophobic Higgs (h_f) at LEP and the Tevatron have yielded negative results so far. In fermiophobic models the decay $H^\pm \rightarrow h_f W^{(*)}$

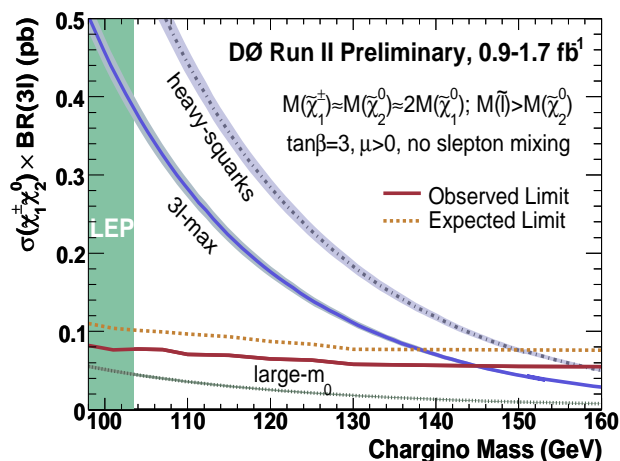


Fig. 6. DØ 95% C.L. limits on the total cross section for associated chargino and neutralino production with leptonic final states as a function of $\chi_{1\pm}$ mass, in comparison with the expectation for several SUSY scenarios. The line corresponds to observed minimal SUGRA limit. PDF and renormalization/factorization scale uncertainties are shown as shaded bands.

can have a larger branching fraction than the conventional decays $H^\pm \rightarrow tb, \tau\nu$. This would lead to double h_f production. Searches have been conducted in the $p\bar{p} \rightarrow h_f H^\pm \rightarrow h_f h_f \rightarrow \gamma\gamma\gamma(\gamma) + X$ production and decay modes by the DØ experiment, leading to $m_{h_f} > 80$ GeV at 95% C.L for $m_{H^\pm} < 100$ GeV and $\tan\beta = 30$. This result represents the first excluded region for a fermiophobic Higgs boson in the class of two Higgs doublets models.

9 Beyond the Standard Model

What do we look for at Tevatron? SUSY and non-SUSY searches can be divided in the following categories:

- enlarged gauge group resulting in exotic Z' or W' bosons.
- alternative electroweak symmetry breaking mechanisms such as technicolor or little Higgs models.
- relationships between quarks and leptons leading to leptoquarks.
- extension beyond the Poincaré group, i.e., supersymmetry.
- increased number of spatial dimensions.
- particle substructure or compositeness, i.e., repeat the history.
- search for excess beyond the standard model without a specific model in mind (signature-based searches).

10 Charginos and Neutralinos

In R -parity-conserving minimal supersymmetric extensions of the standard model, the charged and neutral partners of gauge and Higgs bosons (charginos

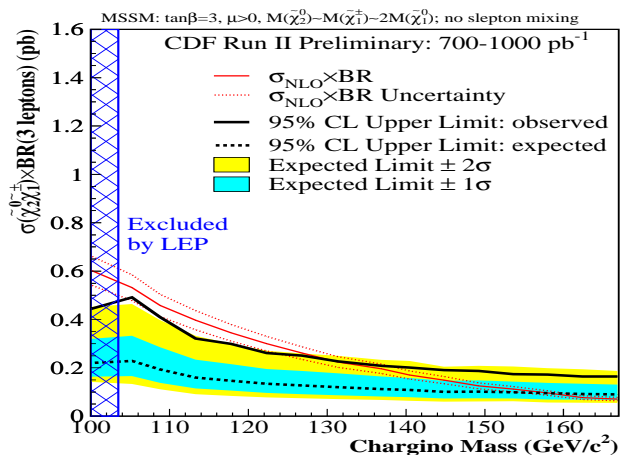


Fig. 7. CDF 95% C.L. limits on the total cross section for associated chargino and neutralino production with leptonic final states. The expected limit corresponds to the dashed line, with $\pm 1\sigma$ and $\pm 2\sigma$ uncertainties bands shown. The next-to-leading order (NLO) production cross section correspond to a model with the universal scalar mass parameter fixed to $m_0 = 70$ GeV with no slepton mixing.

and neutralinos) are produced in pairs and decay into fermions and LSPs. CDF and DØ have searched in the trilepton final state that has long been suggested to be one of the most promising channel for discovery of SUSY at a hadron Collider. However, these searches are very challenging since the cross section are below 0.5 pb, and the leptons are difficult to reconstruct due to their low transverse momenta. Furthermore, many channels need to be combined to achieve sensitivity. The selection consist of two well identified and isolated electrons (e) or muons (μ) with a p_T of the order of 10 GeV. An additional isolated track provides sensitivity to the third lepton (l) and maximizes efficiency by not requiring explicit lepton identification. Some missing transverse energy (\cancel{E}_T) is required, resulting from neutrinos and neutralinos in the final state. Since very few SM processes are capable of generating a pair of isolated like-sign leptons, the same analysis is performed with this looser criterion.

As a guideline, DØ results are interpreted in this model with chargino $\chi_{1\pm}$ and neutralino (χ_2^0, χ_1^0) masses following the relation $m_{\chi_{1\pm}} \simeq m_{\chi_2^0} \simeq 2m_{\chi_1^0}$. Three minimal SUGRA inspired scenarios were used for the interpretation (Fig. 6). Two of them are with enhanced leptonic branching fractions ("heavy squarks" and "3l-max" scenarios). For the 3l-max scenario, the slepton mass is just above the neutralino mass ($m_{\chi_2^0}$), leading to maximum branching fraction into leptons. The heavy squark scenario is characterized by maximal production cross section. Finally, the large universal scalar mass parameter (m_0) scenario is not yet sensitive because the W/Z exchange dominates. The new result from DØ includes an update of the eel channel using 1.7 fb^{-1} . No events are observed after final selection, with 1.0 ± 0.3 event expected. Since no evidence for SUSY is reported, all results are combined to extract limits on the total cross section, taking into ac-

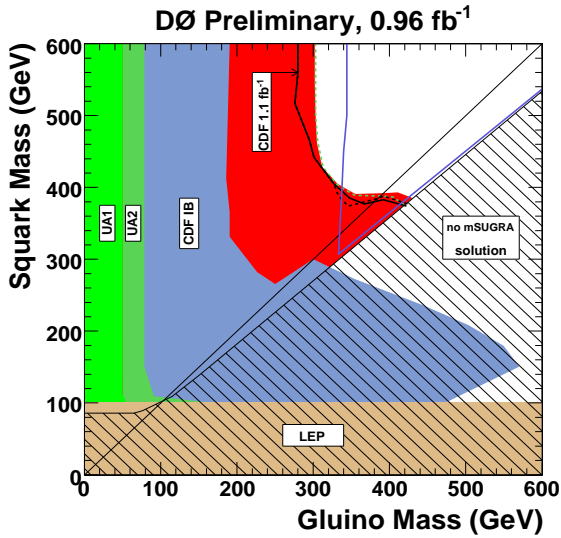


Fig. 8. DØ Run II exclusion plane for squark and gluino masses at 95% C.L using 1 fb^{-1} . The NLO nominal cross section uncertainties are included in the limit calculation. The CDF limits shown on this plot use different model parameters and are thus not directly comparable.

count systematic and statistical uncertainties including their correlations. The DØ combination excludes chargino masses below 145 GeV at 95% C.L for the $3l$ -max scenario.

Similar analyses were performed by CDF but interpreted with slightly different scenarios. The total integrated luminosity corresponds to 1 fb^{-1} , and the resulting cross section limit is shown in Fig. 7 as a function of the chargino mass for the scenario with a fixed value of $m_0 = 70 \text{ GeV}$ and no slepton mixing. This scenario enhances the branching fraction of chargino and neutralino into e or μ , and excludes chargino masses below 129 GeV for a sensitivity (expected limit) of 157 GeV at 95% C.L.

For the interpretation of the results between the two experiments, only the cross section limits can be compared since the fixed low m_0 value leads to a two-body decay for the CDF analysis, while for the DØ analysis a sliding window of m_0 is used to keep the slepton mass slightly above the χ_2^0 mass and corresponds to a three-body decays.

11 Squarks and Gluinos

Squark and gluino production has a large cross section at the Tevatron, with final states of multijet and missing transverse energy (\cancel{E}_T), though searches in these final states have large background. CDF and DØ have searched in three different scenarios. The first is for pair production of squarks, each decaying into a quark and a neutralino, leading to a two jets+ \cancel{E}_T final state. This decay channel is dominant if the gluino is heavier than the squark. The second case is when the squark is heavier than the gluino leading to a final state with 4 jets and \cancel{E}_T . The third case is for

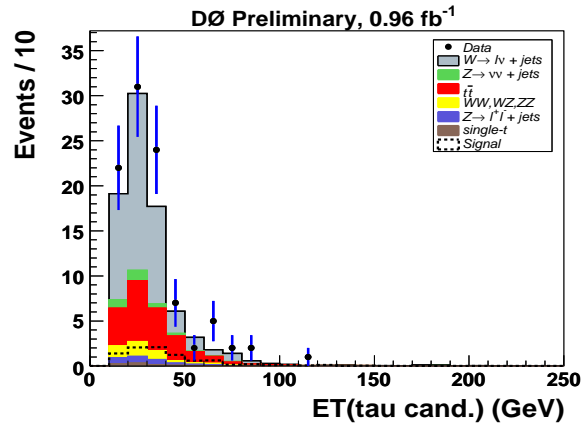


Fig. 9. The transverse energy of tau candidates in the squark pair-production search in events with jets, tau(s) decaying hadronically and large missing transverse energy using all DØ data recorded during the Run IIa phase of the Tevatron.

similar squark and gluino masses, with a final state of three or more jets. Using dedicated multijet+ \cancel{E}_T triggers, and requiring a tight cut on \cancel{E}_T and the scalar p_T sum, cross section upper limits at 95% C.L have been obtained for the sets of minimal SUGRA parameters considered ($\tan \beta = 5(3)$, $A_0 = 0(-2m_0)$, $\mu < 0$ for CDF (DØ)). The data show good agreement with the standard model expectations and mass limits have been derived. The observed and expected limits for DØ using 1 fb^{-1} are shown in Fig.8 as functions of the squark and gluino masses, improving on previous limits. Lower limits of 385 GeV and 302 GeV on the squark and gluino masses, respectively, are derived by DØ at 95% C.L. A complementary search for squarks is performed by DØ in the topology of multijet events accompanied by large missing transverse energy and at least one tau lepton decaying hadronically. The transverse energy of tau candidates is displayed in Fig. 9. Lower limits on the squark mass up to 366 GeV are derived in the framework of minimal supergravity with parameters enhancing final states with taus.

For the third generation, mass unification is broken in many SUSY models due to potentially large mixing effects. This can result in a sbottom or stop with much lower mass than the other squarks and gluinos. DØ has recently updated its analysis of the case where the stop decays with a branching ratio of 100% into a charm quark and a neutralino. Good agreement between the data and the SM prediction is obtained. The derived limits at 95% C.L on the stop mass are shown in Fig. 10. The DØ collaboration has also searched for a light stop in the lepton+jets channel using the stop decay mode $\tilde{t}_1 \rightarrow bW^+\chi_1^0$. Kinematic differences between the stop pair production and the dominant $t\bar{t}$ process are used to separate the two possible contributions. In 1 fb^{-1} , upper cross section limits at 95% C.L on $\tilde{t}_1\tilde{t}_1$ production are a factor of about 7-12 higher than expected for the MSSM model for stop masses ranging between 145-175 GeV.

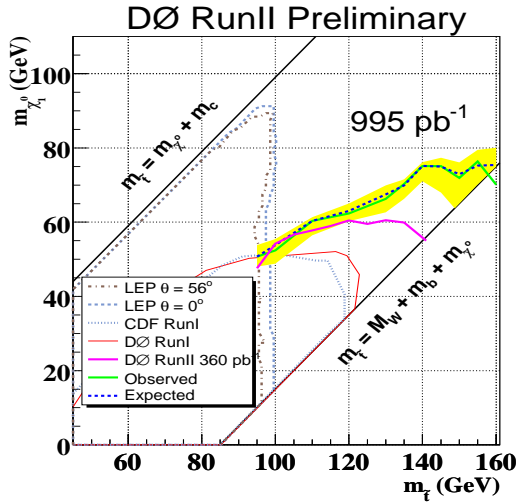


Fig. 10. DØ 95% C.L. exclusion contours in the stop and neutralino mass plane, assuming a stop branching ratio of 100% into a charm and a neutralino.

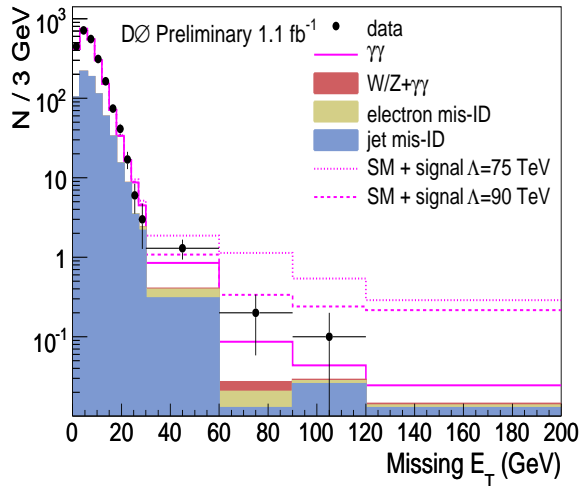


Fig. 11. DØ \cancel{E}_T distribution in $\gamma\gamma$ data with background processes. The expected \cancel{E}_T distribution for GMSB SUSY signal with $\Lambda = 75$ TeV and 90 TeV are presented as dotted and dashed lines, respectively.

12 Gauge Mediated SUSY Breaking

Final states with two photons and \cancel{E}_T can be produced in gauge mediated SUSY breaking models. In the analysis performed by DØ with 1 fb^{-1} , the next-to-lightest supersymmetric particle (NLSP) is assumed to be the lightest neutralino, which decays into a photon and an undetected gravitino. The \cancel{E}_T distributions for the $\gamma\gamma$ sample is given in Fig. 11 with the expected signal contribution for two different values of the effective energy scale Λ of SUSY breaking. After determination of all backgrounds from data, DØ observed no excess of such events and set 95% C.L. limits: the masses of the lightest chargino and neutralino are found to be larger than 231 and 126 GeV, respectively. These are the most restrictive limits to date.

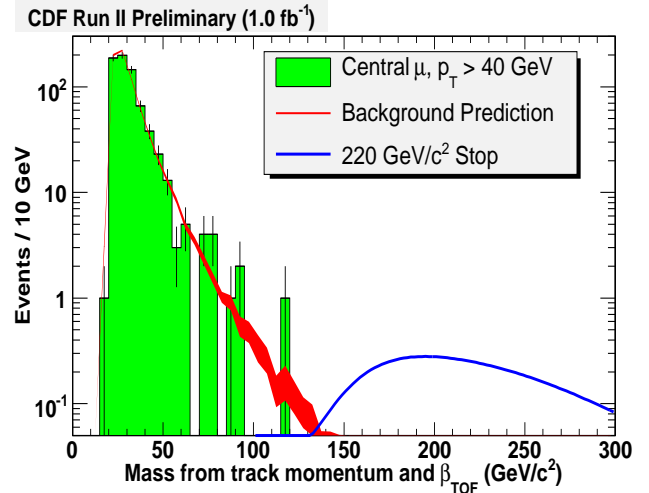


Fig. 12. Mass distribution measured by the time-of-flight of high transverse momentum tracks in events collected by the CDF experiment using high transverse momentum muon trigger. The expected contribution from stable stop pair production is shown for a stop mass of 220 GeV.

13 Long-lived Particles

Several models predict charged or neutral long-lived particles decaying inside or outside the detector. If such a particle is charged [14], it will appear in the detector as a slowly moving, highly ionizing particle with large transverse momentum that will typically be observed in the muon detectors. CDF has performed a model independent search by measuring the time-of-flight using muon triggers. The result is consistent with muon background expectation. Within the context of stable stop pair production, CDF sets a mass limit at 250 GeV at 95% C.L.

14 Leptoquarks

Leptoquarks [15] were postulated to explain many parallels between the families of quarks and leptons. They are predicted in many extensions of the standard model, such as grand unification, superstring, and compositeness models. A search for third generation scalar LQ pair production has been performed in the $\tau b \tau b$ channel using 1 fb^{-1} of data collected at DØ. No evidence of signal has been observed, and limits are set on the production cross section as a function of the leptoquark mass. Assuming β , the branching fraction of the leptoquark into τb , equal to 1, the limit on the mass is 180 GeV at 95% C.L. With a smaller dataset of 0.4 fb^{-1} , assuming a decay into $b\nu$, the limit is 229 GeV. CDF has performed a similar analysis but in the context of vector leptoquarks, which are characterized by higher production cross section, and set a lower mass limit of 251 GeV at 95% C.L. in τb decay.

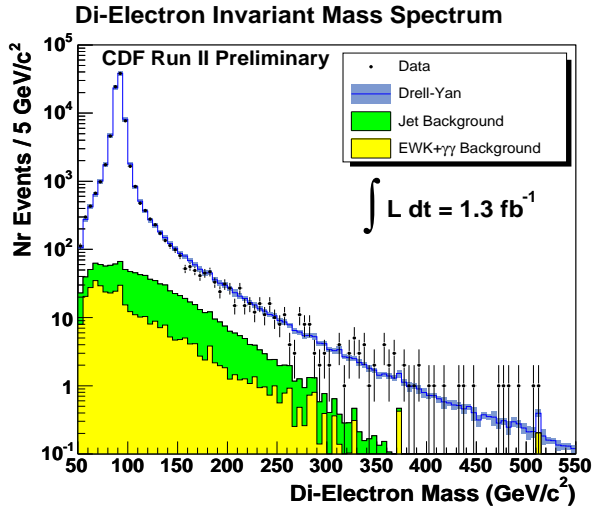


Fig. 13. The di-electron mass measured by CDF with the expected background. There are no observed events above 550 GeV.

15 Extra Gauge Bosons

Extra gauge bosons like Z' are predicted in, e.g., E6 GUTs models [16]. The searches are performed by reconstructing the di-electron mass as shown in Fig. 13. The Z mass peak and the Drell-Yan tail at high mass is well reproduced. By performing a scan for high-mass resonances, CDF sets limits depending on the model. For instance, a lower mass limit of 923 GeV can be set assuming SM-like couplings of the Z' , with a somewhat lower mass limit for E6 Z' bosons.

As for W' decaying into tb , CDF uses a similar analysis as the one for its single top search and provides a limit of 790 GeV at 95% C.L. DØ performed a W' search in the $e\nu$ channel, and set a limit at 965 GeV at 95% C.L., assuming that the new boson has the same couplings to fermions as the standard model W boson.

16 Extra Dimensions

Models postulating the existence of extra spacial dimensions have been proposed to solve the hierarchy problem posed by the large difference between the electroweak symmetry breaking scale at 1 TeV and the Planck scale at which gravity is expected to become strong. The first excited graviton mode predicted by the Randall and Sundrum model [17] could be resonantly produced at the Tevatron. The graviton is expected to decay to fermion-antifermions and to dibosons pairs. CDF and DØ have searched for resonances in their data. Since the graviton has spin 2, the branching fraction to the di-photon final state is expected to be twice that of e^+e^- final states. The background is estimated from misidentified electromagnetic objects and is extracted from the data. Combining the $ee + \gamma\gamma$ final states, limits are set as a function of the graviton mass and the coupling parameter, as represented in Fig. 14.

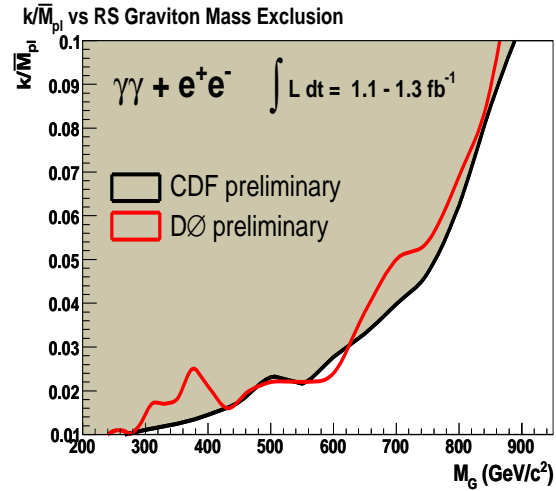


Fig. 14. CDF and DØ 95% C.L. upper limit on k/M_{Planck} versus graviton mass M_G from 1.1-1.3 fb^{-1} of data for the $ee + \gamma\gamma$ final states combined.

17 Signature-Based Searches

A global analysis of CDF Run II data has been carried out to search for indications of new phenomena. Rather than focusing on particular new physics scenarios, CDF data are analyzed for discrepancies with SM prediction. A model-independent approach (Vista) focuses on obtaining a panoramic view of the entire data landscape, and is sensitive to new large-cross-section physics. A quasi-model-independent approach (Sleuth) emphasizes the high- p_T tails, and is particularly sensitive to new electroweak scale physics. A subset of the Vista comparison is given in Table. 3. This global search for new physics in 1 fb^{-1} of $p\bar{p}$ collisions reveals no indication of physics beyond the SM.

A separate CDF analysis in the $\cancel{E}_T + \text{photon} + \text{lepton}$ final state using 1 fb^{-1} of Run II data has not confirmed the Run I excess.

18 Conclusion

The Tevatron Run II collider program is scheduled to run through mid-2009 with possibility of extending into 2010 to add an extra 25% of data, leading to an expected delivered integrated luminosity of $\approx 8.6 \text{fb}^{-1}$. The accelerator performance is excellent and provides a great opportunity for the CDF and DØ experiments to meet or exceed their stated physics goals. The search for the Higgs boson and physics beyond the standard model will greatly benefit from this additional integrated luminosity.

19 Acknowledgments

I would like to thank my colleagues at CDF and DØ, especially those who construct, maintain, and calibrate the detectors, essential for any physics analysis reported here. I wish also to thank all the colleagues

Table 3. A subset of the model-independent search (Vista), which compares CDF Run II data with the SM prediction. Events are partitioned into exclusive final states based on standard CDF particle identification criteria. Final states are labeled in this table according to the number and types of objects present, and are ordered according to decreasing discrepancy between the total number of events expected and the total number observed in the data. Only statistical uncertainties on the background prediction have been included in this Table.

CDF Run II Preliminary (927 pb ⁻¹)								
Final State	Data	Background	Final State	Data	Background	Final State	Data	Background
3j τ +	71	113.7 \pm 3.6	2e+j	13	9.8 \pm 2.2	e+ γ \not{p}	141	144.2 \pm 6
5j	1661	1902.9 \pm 50.8	2e+e-	12	4.8 \pm 1.2	e+ μ - \not{p}	54	42.6 \pm 2.7
2j τ +	233	296.5 \pm 5.6	2e+	23	36.1 \pm 3.8	e+ μ + \not{p}	13	10.9 \pm 1.3
be+j	2207	2015.4 \pm 28.7	2b $\Sigma p_T > 400$ GeV	327	335.8 \pm 7	e+ μ -	153	127.6 \pm 4.2
3j $\Sigma p_T < 400$ GeV	35436	37294.6 \pm 524.3	2b $\Sigma p_T < 400$ GeV	187	173.1 \pm 7.1	e+j	386880	392614 \pm 5031.8
e+3j \not{p}	1954	1751.6 \pm 42	2b3j $\Sigma p_T < 400$ GeV	28	33.5 \pm 5.5	e+j2 γ	14	15.9 \pm 2.9
be+2j	798	695.3 \pm 13.3	2b2j $\Sigma p_T > 400$ GeV	355	326.3 \pm 8.4	e+j τ +	79	79.3 \pm 2.9
3j \not{p} $\Sigma p_T > 400$ GeV	811	967.5 \pm 38.4	2b2j $\Sigma p_T < 400$ GeV	56	80.2 \pm 5	e+j τ -	162	148.8 \pm 7.6
e+ μ +	26	11.6 \pm 1.5	2b2j γ	16	15.4 \pm 3.6	e+j \not{p}	58648	57391.7 \pm 661.6
e+ γ	636	551.2 \pm 11.2	2b γ	37	31.7 \pm 4.8	e+j γ \not{p}	52	76.2 \pm 9
e+3j	28656	27281.5 \pm 405.2	2bj $\Sigma p_T > 400$ GeV	415	393.8 \pm 9.1	e+j μ - \not{p}	22	13.1 \pm 1.7
b5j	131	95 \pm 4.7	2bj $\Sigma p_T < 400$ GeV	161	195.8 \pm 8.3	e+j μ -	28	26.8 \pm 2.3
j2 τ +	50	85.6 \pm 8.2	2bj \not{p} $\Sigma p_T > 400$ GeV	28	23.2 \pm 2.6	e+e-4j	103	113.5 \pm 5.9
j τ + τ -	74	125 \pm 13.6	2bj γ	25	24.7 \pm 4.3	e+e-3j	456	473 \pm 14.6
b \not{p} $\Sigma p_T > 400$ GeV	10	29.5 \pm 4.6	2be+2j \not{p}	15	12.3 \pm 1.6	e+e-2j \not{p}	30	39 \pm 4.6
e+j γ	286	369.4 \pm 21.1	2be+2j	30	30.5 \pm 2.5	e+e-2j	2149	2152 \pm 40.1
e+j \not{p} τ -	29	14.2 \pm 1.8	2be+j	28	29.1 \pm 2.8	e+e- τ +	14	11.1 \pm 2
2j $\Sigma p_T < 400$ GeV	96502	92437.3 \pm 1354.5	2be+	48	45.2 \pm 3.7	e+e- \not{p}	491	487.9 \pm 12
be+3j	356	298.6 \pm 7.7	τ + τ -	498	428.5 \pm 22.7	e+e- γ	127	132.3 \pm 4.2
8j	11	6.1 \pm 2.5	γ τ +	177	204.4 \pm 5.4	e+e-j	10726	10669.3 \pm 123.5
7j	57	35.6 \pm 4.9	γ \not{p}	1952	1945.8 \pm 77.1	e+e-j \not{p}	157	144 \pm 11.2
6j	335	298.4 \pm 14.7	μ + τ +	18	19.8 \pm 2.3	e+e-j γ	26	45.6 \pm 4.7
4j $\Sigma p_T > 400$ GeV	39665	40898.8 \pm 649.2	μ + τ -	151	179.1 \pm 4.7	e+e-	58344	58575.6 \pm 603.9
4j $\Sigma p_T < 400$ GeV	8241	8403.7 \pm 144.7	μ + \not{p}	321351	320500 \pm 3475.5	b6j	24	15.5 \pm 2.3
4j2 γ	38	57.5 \pm 11	μ + \not{p} τ -	22	25.8 \pm 2.7	b4j $\Sigma p_T > 400$ GeV	13	9.2 \pm 1.8
4j τ +	20	36.9 \pm 2.4	μ + γ	269	285.5 \pm 5.9	b4j $\Sigma p_T < 400$ GeV	464	499.2 \pm 12.4
4j \not{p} $\Sigma p_T > 400$ GeV	516	525.2 \pm 34.5	μ + γ \not{p}	269	282.2 \pm 6.6	b3j $\Sigma p_T > 400$ GeV	5354	5285 \pm 72.4
4j γ \not{p}	28	53.8 \pm 11	μ + μ - \not{p}	49	61.4 \pm 3.5	b3j $\Sigma p_T < 400$ GeV	1639	1558.9 \pm 24.1
4j γ	3693	3827.2 \pm 112.1	μ + μ - γ	32	29.9 \pm 2.6	b3j \not{p} $\Sigma p_T > 400$ GeV	111	116.8 \pm 11.2
4j μ +	576	568.2 \pm 26.1	μ + μ -	10648	10845.6 \pm 96	b3j γ	182	194.1 \pm 8.8
4j μ + \not{p}	232	224.7 \pm 8.5	j2 γ	2196	2200.3 \pm 35.2	b3j μ + \not{p}	37	34.1 \pm 2
4j μ + μ -	17	20.1 \pm 2.5	j2 γ \not{p}	38	27.3 \pm 3.2	b3j μ +	47	52.2 \pm 3
3 γ	13	24.2 \pm 3	j τ +	563	585.7 \pm 10.2	b2 γ	15	14.6 \pm 2.1
3j $\Sigma p_T > 400$ GeV	75894	75939.2 \pm 1043.9	j \not{p} $\Sigma p_T > 400$ GeV	4183	4209.1 \pm 56.1	b2j $\Sigma p_T > 400$ GeV	8812	8576.2 \pm 97.9
3j2 γ	145	178.1 \pm 7.4	j γ	49052	48743 \pm 546.3	b2j $\Sigma p_T < 400$ GeV	4691	4646.2 \pm 57.7
3j \not{p} $\Sigma p_T < 400$ GeV	20	30.9 \pm 14.4	j γ τ +	106	104 \pm 4.1	b2j \not{p} $\Sigma p_T > 400$ GeV	198	209.2 \pm 8.3
3j γ τ +	13	11 \pm 2	j γ \not{p}	913	965.2 \pm 41.5	b2j γ	429	425.1 \pm 13.1
3j γ \not{p}	83	102.9 \pm 11.1	j μ +	33462	34026.7 \pm 510.1	b2j μ + \not{p}	46	40.1 \pm 2.7
3j γ	11424	11506.4 \pm 190.6	j μ + τ -	29	37.5 \pm 4.5	b2j μ +	56	60.6 \pm 3.4
3j μ + \not{p}	1114	1118.7 \pm 27.1	j μ + \not{p} τ -	10	9.6 \pm 2.1	b τ +	19	19.9 \pm 2.2
3j μ + μ -	61	84.5 \pm 9.2	j μ + \not{p}	45728	46316.4 \pm 568.2	b γ	976	1034.8 \pm 15.6
3j μ +	2132	2168.7 \pm 64.2	j μ + γ \not{p}	78	69.8 \pm 9.9	b γ \not{p}	18	16.7 \pm 3.1
3bj $\Sigma p_T > 400$ GeV	14	9.3 \pm 1.9	j μ + γ	70	98.4 \pm 12.1	b μ +	303	263.5 \pm 7.9
2 τ +	316	290.8 \pm 24.2	j μ + μ -	1977	2093.3 \pm 74.7	b μ + \not{p}	204	218.1 \pm 6.4
2 γ \not{p}	161	176 \pm 9.1	e+4j	7144	6661.9 \pm 147.2	bj $\Sigma p_T > 400$ GeV	9060	9275.7 \pm 87.8
2 γ	8482	8349.1 \pm 84.1	e+4j \not{p}	403	363 \pm 9.9	bj $\Sigma p_T < 400$ GeV	7236	7030.8 \pm 74
2j $\Sigma p_T > 400$ GeV	93408	92789.5 \pm 1138.2	e+3j τ -	11	7.6 \pm 1.6	bj2 γ	13	17.6 \pm 3.3
2j2 γ	645	612.6 \pm 18.8	e+3j γ	27	21.7 \pm 3.4	bj τ +	13	12.9 \pm 1.8
2j τ + τ -	15	25 \pm 3.5	e+2 γ	47	74.5 \pm 5	bj \not{p} $\Sigma p_T > 400$ GeV	53	60.4 \pm 19.9
2j \not{p} $\Sigma p_T > 400$ GeV	74	106 \pm 7.8	e+2j	126665	122457 \pm 1672.6	bj γ	937	989.4 \pm 20.6
2j \not{p} $\Sigma p_T < 400$ GeV	43	37.7 \pm 100.2	e+2j τ -	53	37.3 \pm 3.9	bj γ \not{p}	34	30.5 \pm 4
2j γ	33684	33259.9 \pm 397.6	e+2j τ +	20	24.7 \pm 2.3	bj μ + \not{p}	104	112.6 \pm 4.4
2j γ τ +	48	41.4 \pm 3.4	e+2j \not{p}	12451	12130.1 \pm 159.4	bj μ +	173	141.4 \pm 4.8
2j γ \not{p}	403	425.2 \pm 29.7	e+2j γ	101	88.9 \pm 6.1	be+3j \not{p}	68	52.2 \pm 2.2
2j μ + \not{p}	7287	7320.5 \pm 118.9	e+ τ -	609	555.9 \pm 10.2	be+2j \not{p}	87	65 \pm 3.3
2j μ + γ \not{p}	13	12.6 \pm 2.7	e+ τ +	225	211.2 \pm 4.7	be+ \not{p}	330	347.2 \pm 6.9
2j μ + γ	41	35.7 \pm 6.1	e+ \not{p}	476424	479572 \pm 5361.2	be+j \not{p}	211	176.6 \pm 5
2j μ + μ -	374	394.2 \pm 24.8	e+ \not{p} τ -	48	35 \pm 2.7	be+e-j	22	34.6 \pm 2.6
2j μ +	9513	9362.3 \pm 166.8	e+ \not{p} τ +	20	18.7 \pm 1.9	be+e-	62	55 \pm 3.1

for providing the material for this presentation as well as the organizers of the SUSY 2007 conference, in particular Wim de Boer and Dieter Zeppenfeld, for this well-organized, successful and enjoyable event.

References

1. P. W. Higgs, *Phys. Lett.* **12**, 132 (1964).
2. H.E. Haber and G.L. Kane, *Phys. Rep.* **117**, 75 (1985).
3. H.P. Nilles, *Phys. Rep.* **110**, 1 (1984).

4. Slides: <http://indico.cern.ch/getFile.py/access?contribId=82&sessionId=146&resId=1&materialId=slides&confId=6210>
5. CDF Collaboration, CDF physics results page: <http://www-cdf.fnal.gov/physics/physics.html>
6. D \bar{O} Collaboration, D \bar{O} physics results page: <http://www-d0.fnal.gov/Run2Physics/WWW/results.htm>
7. CDF Collaboration, *Phys. Rev.* **D71**, 032001 (2005).
8. D \bar{O} Collaboration, *Nucl. Instrum. Methods* **A565**, 463 (2006).
9. LEP Electroweak Working Group, <http://lepewwg.web.cern.ch/LEPEWWG/>
10. LEP Collaborations, *Phys. Lett.* **B565**, 61 (2003).

11. M. Carena, S. Heinemeyer, C. E. M. Wagner, and G. Weiglein, *Eur. Phys. J.* **C26**, 601-607 (2003).
12. G. B. Gelmini and M. Roncadelli, *Phys. Lett.* **B99**, 411 (1981).
13. N. Arkani-Hamed, A. G. Cohen, E. Katz, and A. E. Nelson, *J. High Energy Phys.* **0207**, 034 (2002).
14. A. De Rujula, S. L. Glashow, and U. Sarid, *Nucl. Phys.* **B333**, 173 (1990).
15. W. Buchmuller and D. Wyler, *Phys. Lett.* **B177**, 377 (1986).
16. P. Langacker, R. W. Robinett, and J.L. Rosner, *Phys. Rev.* **D30**, 1470 (1984).
17. L. Randall and R. Sundrum, *Phys. Rev. Lett.* **83**, 3370 (1999); *ibid.*, **83**, 4690 (1999).